SIAM J. SCI. COMPUT.
Vol. 43, No. 1, pp. A309–A329

AN EFFICIENT SPECTRAL METHOD FOR ELLIPTIC PDES IN COMPLEX DOMAINS WITH CIRCULAR EMBEDDING*

YIQI GU† AND JIE SHEN†

Abstract. We apply the fictitious domain concept with circular embedding to solve elliptic boundary value problems in domains of complex geometry. Different from the usual approach with rectangular embedding, the circular embedding enables us to transform two-dimensional problems in complex domains to a sequence of one-dimensional problems that can be efficiently solved by a spectral Petrov–Galerkin formulation. It is shown, at least in the special case, that this method is well-posed along with error estimates indicating spectral convergence. Ample numerical results are presented to demonstrate the effectiveness of this approach for problems with smooth solutions as well as singular solutions.

Key words. spectral method, fictitious domain, elliptic PDE, error estimate

AMS subject classifications. 65N15, 65N35, 65N85

DOI. 10.1137/20M1345153

1. Introduction.

Spectral methods have become a major computational tool in solving PDEs thanks to their high accuracy for problems with smooth solutions. However, their applicability has been mostly limited to problems posed in regular geometries. For problems in complex geometries, there are essentially two approaches that are amenable to spectral methods: (i) map the complex domain into a regular domain through an explicit, smooth mapping [26] or through the Gordon–Hall mapping [19] and (ii) embed the complex domain into a larger regular domain, which belongs to the class of fictitious domain methods. The first approach is limited to problems with smooth (or a fixed number of piecewise smooth) boundaries that can be mapped to regular domains with explicit mapping and will lead to a transformed PDE with complicated variable coefficients. So we shall concentrate on the second approach in this paper.

There have been various attempts in using the fictitious domain approach to solve PDEs in complex domains. Examples include adding a penalty term to the extended equations [5, 27, 32], introducing Lagrange multipliers on the boundary [12, 18, 33], diffuse domain method [10, 11, 22], boundary integral method [8, 15, 6] etc. The main drawbacks of these methods are their low order of convergence rate even for smooth solutions and, in the case of spectral methods, high computational cost [33, 13, 14, 17]. The Fourier extension method [9, 24, 23] has been shown to be very effective for parabolic-type PDEs, and elliptic-type PDEs can be solved as steady-state solutions of parabolic-type PDEs.

In a recent work [20], we presented our first attempt in using spectral methods to solve 2-D second-order elliptic PDEs by enclosing the original complex domains into a larger rectangular domain. Two types of Petrov–Galerkin formulations with

*Submitted to the journal's Methods and Algorithms for Scientific Computing section June 12, 2020; accepted for publication (in revised form) November 30, 2020; published electronically January 20, 2021.

https://doi.org/10.1137/20M1345153

Funding: This work was partially supported by NSF grant DMS-1720442 and AFOSR grant FA9550-16-1-0102.

†Department of Mathematics, Purdue University, 150 N. University Street, West Lafayette, IN 47907-2067 USA (gu129@purdue.edu, shen7@purdue.edu).

special trial and test functions are constructed. One is suitable only for the Poisson equation. The other works for general elliptic equations, but its well-posedness is still not available. Both algorithms require solving a $O(NM) \times O(NM)$ sparse linear system, where N and M are, respectively, the degrees of freedom in the x- and y-direction.

In this paper, we present a more efficient and well-posed spectral method using a circular embedding. The main advantage of this approach is that by using the polar transformation, the extended 2-D problem can be decomposed into a sequence of 1-D differential equations with an undetermined boundary condition at the artificial boundary. These boundary conditions are determined by the original boundary condition of the PDE through a least-square formulation. More precisely, this approach only needs to solve a sequence of $N \times N$ sparse linear systems, where N is the degree of freedom in the r-direction, and a $2M \times 2M$ full linear system, where M is the number of degree of freedom in the θ-direction. Compared to the method in [20], it is more efficient and much simpler to implement. Moreover, at least for a special case, the well-posedness and error estimates can be rigorously established.

The rest of the paper is organized as follows. In section 2, we describe the fictitious domain formulation with a circular embedding, build the extended problem, and describe the whole algorithm in both the spatial continuous and discrete cases. In section 3, we carry out a rigorous error analysis for a special case. In section 4, we present several numerical examples to demonstrate the convergence rate for various problems. Extension to 3-D problems is presented in section 5, followed by some concluding remarks in section 6.

We first present some of the notations to be used in what follows. We define the scaled Jacobi weight function,

$$\hat{\omega}^{\alpha,\beta}(r) = (1-r)^{\alpha} r^{\beta}, \tag{1.1}$$

and the weighted L^2 inner product,

$$(u, v)_{\hat{\omega}^{\alpha,\beta}} = \int_0^1 u(r)\bar{v}(r)\hat{\omega}^{\alpha,\beta}(r)\mathrm{d}r. \tag{1.2}$$

The corresponding weighted L^2 and H^1 spaces are defined by

$$L^2_{\hat{\omega}^{\alpha,\beta}} = \left\{ u(r) : \int_0^1 |u(r)|^2 \hat{\omega}^{\alpha,\beta}(r)\mathrm{d}r < \infty \right\}, \tag{1.3}$$

$$H^1_{\hat{\omega}^{\alpha,\beta}} = \left\{ u(r) : u, \partial_r u \in L^2_{\hat{\omega}^{\alpha,\beta}} \right\}, \tag{1.4}$$

equipped with norms

$$\|u\|_{\hat{\omega}^{\alpha,\beta}} = \left(\int_0^1 |u(r)|^2 \hat{\omega}^{\alpha,\beta}(r)\mathrm{d}r \right)^{\frac{1}{2}}, \tag{1.5}$$

$$\|u\|_{1,\hat{\omega}^{\alpha,\beta}} = \left(\|u\|^2_{\hat{\omega}^{\alpha,\beta}} + \|\partial_r u\|^2_{\hat{\omega}^{\alpha,\beta}} \right)^{\frac{1}{2}}. \tag{1.6}$$

In particular, we set $(\cdot,\cdot) = (\cdot,\cdot)_{\hat{\omega}^{0,0}}$ $\|\cdot\| = \|\cdot\|_{\hat{\omega}^{0,0}}$.

Let $\Pi := (0,1) \times [0, 2\pi)$; we introduce the space $H^{1,s}_{\mathrm{p}}(\Pi)$ with $s \geq 0$, which contains functions defined in Π that are 2π-periodic with respect to θ, with the norm defined by

$$\|u\|_{H^{1,s}_{\mathrm{p}}(\Pi)} = \left(\sum_{|m|=0}^{\infty} m^{2s} \left(m^2 \|u^m\|^2_{\hat{\omega}^{0,-1}} + \|\partial_r u^m\|^2_{\hat{\omega}^{0,1}} \right) \right)^{\frac{1}{2}}, \tag{1.7}$$

assuming u can be expanded by

$$u(r,\theta) = \sum_{|m|=0}^{\infty} u^m(r) e^{\mathrm{i}m\theta}. \tag{1.8}$$

More precisely, $u(r,\theta) \in H^{1,s}_{\mathrm{p}}(\Pi)$ if and only if $u^m(r) \in H^1_{\hat{\omega}^{0,1}} \cap L^2_{\hat{\omega}^{0,-1}}$ and $\sum_{|m|=0}^{\infty} m^{2s}(m^2\|u^m\|^2_{\hat{\omega}^{0,-1}} + \|\partial_r u^m\|^2_{\hat{\omega}^{0,1}}) < \infty$. We also define the non-uniformly weighted Sobolev space

$$\hat{B}^s_{\alpha,\beta} = \left\{ u(r) : \partial_r^k u \in L^2_{\hat{\omega}^{\alpha+k,\beta+k}}, \quad 0 \le k \le s \right\}. \tag{1.9}$$

2. Problem formulation and its approximation. We shall first describe the formulation with circular embedding and its decomposition using the polar transform. Then, we present the precise Petrov–Galerkin formulation in both spatial continuous and discrete cases.

2.1. Problem formulation and a conceptual algorithm. We consider the following Poisson-type problem:

$$\begin{aligned} \alpha V - \Delta V &= F \quad \text{in } \Omega, \\ V &= H \quad \text{on } \partial\Omega, \end{aligned} \tag{2.1}$$

where $\alpha \ge 0$; Ω is a 2-D simply connected smooth domain; $F \in C(\overline{\Omega})$; $H \in C(\partial\Omega)$. Let $\widetilde{\Omega}$ be a circular domain that encloses Ω, namely, $\Omega \subset\subset \widetilde{\Omega}$ (see Figure 2.1), and assume that F is extended smoothly from Ω to $\widetilde{\Omega}$. Smooth extensions (or continuations) of given functions have been well studied. For examples, the extension by using truncated Fourier series in 1-D cases is developed in [7, 23, 2], and the Fourier extension in high-dimensional cases can be implemented by performing 1-D extension on each direction [9, 24, 3, 4]. We assume in the following a smooth extension can always be performed on F. Thereafter if U solves the following extended problem in $\widetilde{\Omega}$,

$$\begin{aligned} \alpha U - \Delta U &= F \quad \text{in } \widetilde{\Omega}, \\ U &= H \quad \text{on } \partial\Omega, \end{aligned} \tag{2.2}$$

we have $U|_\Omega = V$. Hence, we only need to solve the extended problem (2.2). It is worth noting that the convergence of the method can be affected by the chosen

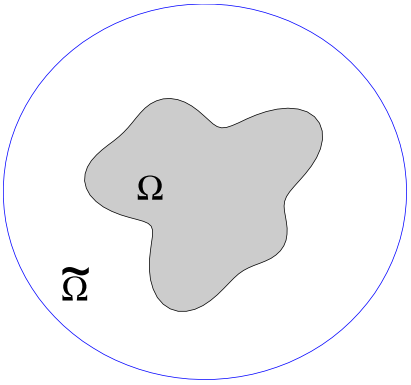

FIG. 2.1. *The original domain* Ω *and the enclosing circle* $\widetilde{\Omega}$.

extension technique [7]. However, it is not clear in what sense the above problem is well-posed. Unlike traditional approaches in which one starts with a well-posed weak formulation and then constructs corresponding numerical algorithms, we shall first construct a feasible algorithm through a dimension reduction and then find a suitable weak formulation that corresponds to the algorithm.

Without loss of generality, we assume in the following $\widetilde{\Omega} = \{(x, y) : x^2 + y^2 < 1\}$, which is the interior of the unit circle. By applying the polar transform,

$$\mathbb{T} : \overline{\Pi} \to \overline{\widetilde{\Omega}}, \quad \mathbb{T}(r, \theta) = (r\cos\theta, r\sin\theta), \tag{2.3}$$

to (2.2) and denoting

$$u(r,\theta) := U(r\cos\theta, r\sin\theta),\ f(r,\theta) := F(r\cos\theta, r\sin\theta),\ h(r,\theta) := H(r\cos\theta, r\sin\theta),$$

we have

$$\begin{aligned} &\alpha u - \frac{1}{r}(ru_r)_r - \frac{1}{r^2}u_{\theta\theta} = f, \quad (r,\theta) \in \Pi; \\ &u_\theta(0,\theta) = 0, \quad u \text{ is periodic in } \theta; \\ &u = h \text{ on } \Gamma; \end{aligned} \tag{2.4}$$

where $\Gamma = \mathbb{T}^{-1}(\partial\Omega)$ is the preimage of $\partial\Omega$. Next, we apply the Fourier transform in θ direction to reduce the 2-D problem (2.4) to a sequence of 1-D problems. More precisely, expanding u and f as

$$u(r,\theta) = \sum_{|m|=0}^{\infty} u^m(r) e^{\mathrm{i}m\theta}, \tag{2.5}$$

$$f(r,\theta) = \sum_{|m|=0}^{\infty} f^m(r) e^{\mathrm{i}m\theta} \tag{2.6}$$

and substituting (2.5) and (2.6) into (2.4), we find that $u^m(r)$ are determined by a sequence of Bessel-type ODEs

$$-\frac{1}{r}\partial_r(r\partial_r u^m) + \left(\frac{m^2}{r^2} + \alpha\right) u^m = f^m(r), \quad 0 < r < 1, \tag{2.7}$$

with one-sided pole conditions

$$u^m(0) = 0 \quad \text{if } m \neq 0. \tag{2.8}$$

Note that the system (2.7)–(2.8) is undetermined since there is no boundary condition at $r = 1$. To arrive at a well-posed system for u^m, we propose to add an artificial boundary condition

$$u^m(1) = t^m \tag{2.9}$$

with t^m to be determined. Given t^m, the solution $u^m(r)$ can be explicitly derived as follows. Let $\{\phi^m\}$ be the solution of

$$\begin{aligned} &-\frac{1}{r}\partial_r(r\partial_r\phi^m) + \left(\frac{m^2}{r^2} + \alpha\right)\phi^m = 0, \quad 0 < r < 1, \\ &\phi^m(0) = 0 \quad \text{if } m \neq 0, \quad \phi^m(1) = 1, \end{aligned} \tag{2.10}$$

and $\{\psi^m\}$ be the solution of

$$
\begin{aligned}
&-\frac{1}{r}\partial_r(r\partial_r\psi^m)+\left(\frac{m^2}{r^2}+\alpha\right)\psi^m=f^m, \quad 0<r<1,\\
&\psi^m(0)=0 \quad \text{if } m\neq 0, \quad \psi^m(1)=0.
\end{aligned} \tag{2.11}
$$

Then, it is easy to see that we have

$$
u^m(r;t^m)=t^m\phi^m(r)+\psi^m(r). \tag{2.12}
$$

It can be verified that the solutions of (2.10) have the following expression:

$$
\phi^m(r)=\begin{cases} r^{|m|}, & \alpha=0,\\ \frac{I_{|m|}(\sqrt{\alpha}r)}{I_{|m|}(\sqrt{\alpha})}, & \alpha>0 \end{cases} \tag{2.13}
$$

for all m, where $I_{|m|}(z)$ are the modified Bessel functions of the first kind [1]. As for (2.11), we can solve it efficiently with a spectral-Galerkin approximation described in [29].

It remains to determine $\{t^m\}$. The key is to choose $\{t^m\}$ such that $u=h$ on Γ. Specifically, suppose Γ is star-shaped and parametrized by

$$
\Gamma=\{(\rho(\theta),\theta):0\le\theta<2\pi\}; \tag{2.14}
$$

we find that $u=h$ on Γ is equivalent to

$$
\int_0^{2\pi} u(\rho(\theta),\theta)\overline{\xi(\theta)}\mathrm{d}\theta=\int_0^{2\pi} h(\rho(\theta),\theta)\overline{\xi(\theta)}\mathrm{d}\theta \quad \forall\xi(\theta)\in L^2[0,2\pi). \tag{2.15}
$$

Using (2.5) and (2.12) and taking $\xi(\theta)=e^{\mathrm{i}k\theta}$, we find from the above that

$$
\sum_{|m|=0}^{\infty}\int_0^{2\pi}\left(t^m\phi^m(\rho(\theta))+\psi^m(\rho(\theta))\right)e^{\mathrm{i}(m-k)\theta}\mathrm{d}\theta=\int_0^{2\pi}h(\rho(\theta),\theta)e^{-\mathrm{i}k\theta}\mathrm{d}\theta \quad \forall|k|=0,1,2,\ldots. \tag{2.16}
$$

Remark 2.1. For more general boundaries Γ, e.g., the boundary of complicated polygonal shapes, it can be parametrized by $\Gamma=\{(\rho(t),\theta(t)):0\le t<1\}$, and an equation similar to (2.16) can be formulated.

2.2. Continuous Petrov–Galerkin formulation. We derive below the Petrov–Galerkin formulation corresponding to the method described in section 2 for the extended 2-D problem (2.4). We define 1-D Hilbert spaces by

$$
\begin{aligned}
\hat{W}^0&=\left\{u(r):\int_0^1(|u|^2+|\partial_r u|^2)r\,\mathrm{d}r<\infty\right\},\\
\hat{W}^m&=\left\{u(r):u(0)=0,\int_0^1\frac{m^2}{r}|u|^2+r|\partial_r u|^2\mathrm{d}r<\infty\right\}, \quad m\neq 0,\\
\hat{Y}^m&=\{u\in\hat{W}^m:u(1)=0\} \quad \forall m,
\end{aligned} \tag{2.17}
$$

equipped with the following norms:

$$
\|u\|_{\hat{W}^m}:=\begin{cases}\left(\|u\|^2_{\hat{\omega}^{0,1}}+\|\partial_r u\|^2_{\hat{\omega}^{0,1}}\right)^{\frac{1}{2}}, & m=0,\\ \left(m^2\|u\|^2_{\hat{\omega}^{0,-1}}+\|\partial_r u\|^2_{\hat{\omega}^{0,1}}\right)^{\frac{1}{2}}, & m\neq 0.\end{cases} \tag{2.18}
$$

Then we define

$$W := \left\{ u(r,\theta) = \sum_{|m|=0}^{\infty} u^m(r) e^{\mathrm{i}m\theta} : u^m \in \hat{W}^m, \ \sum_{|m|=0}^{\infty} \|u^m\|^2_{\hat{W}^m} < \infty \right\} \tag{2.19}$$

with norm

$$\|u\|_W := \left(\sum_{|m|=0}^{\infty} \|u^m\|^2_{\hat{W}^m} \right)^{\frac{1}{2}}. \tag{2.20}$$

We also define a bilinear form $A(\cdot,\cdot) : W \times W \to \mathbb{C}$ by

$$A(u,v) := \sum_{|m|=0}^{\infty} m^2 (u^m, v^m)_{\hat{\omega}^{0,-1}} + (\partial_r u^m, \partial_r v^m)_{\hat{\omega}^{0,1}} + \alpha (u^m, v^m)_{\hat{\omega}^{0,1}}. \tag{2.21}$$

Next, we define the trial space by

$$X := \left\{ u \in W : u|_\Gamma = h \right\} \tag{2.22}$$

and the test space by

$$Y := \left\{ v \in W : v(r,\theta) = \sum_{|m|=0}^{\infty} v^m(r) e^{\mathrm{i}m\theta} \text{ with } v^m \in \hat{Y}^m \right\} \tag{2.23}$$

and consider the following weak formulation:

$$\begin{cases} \text{Find } u \in X \text{ such that} \\ A(u,v) = (rf, v) \quad \forall v \in Y. \end{cases} \tag{2.24}$$

We show below that any solution of the algorithm constructed in the last subsection is a solution of the above weak problem.

PROPOSITION 2.1. *Let* $\{\phi^m\}$, $\{\psi^m\}$ *be the solutions of* (2.10) *and* (2.11), *and let* $u^m = t^m \phi^m(r) + \psi^m(r)$ *with* $\{t^m\}$ *satisfying* (2.16). *Then* $u(r,\theta) = \sum_{|m|=0}^{\infty} u^m(r) e^{im\theta}$ *is a solution of* (2.24).

Proof. It is clear that each $u^m = t^m \phi^m(r) + \psi^m(r)$ satisfies (2.7) with $u^m(1) = t^m$ and $u^m \in \hat{W}^m$. Hence $u(r,\theta) = \sum_{|m|=0}^{\infty} u^m(r) e^{im\theta} \in W$. For any $v = \sum_{|m|=0}^{\infty} v^m(r)$ $e^{\mathrm{i}m\theta} \in Y$, we multiply v^m on both sides of (2.7) and integrate by parts to obtain

$$m^2 (u^m, v^m)_{\hat{\omega}^{0,-1}} + (\partial_r u^m, \partial_r v^m)_{\hat{\omega}^{0,1}} + \alpha (u^m, v^m)_{\hat{\omega}^{0,1}} = (f^m, v^m)_{\hat{\omega}^{0,1}}. \tag{2.25}$$

Sum up (2.25) for $|m| = 0, 1, \ldots$; it directly follows that $A(u,v) = (rf, v)$.

It remains to show $u \in X$. Indeed, we derive from (2.16) that $u(\rho(\theta),\theta) = h(\rho(\theta),\theta)$, which implies $u \in X$. Hence, u is a solution of (2.24). ∎

The well-posedness of (2.24) in the general case is not easy. We can show that $A(\cdot,\cdot)$ is continuous in $W \times W$. Indeed,

(2.26)
$$\begin{aligned}|A(u,v)| &\le \sum_{|m|=0}^{\infty} m^2 |(u^m, v^m)_{\hat{\omega}^{0,-1}}| + |(\partial_r u^m, \partial_r v^m)_{\hat{\omega}^{0,1}}| + \alpha |(u^m, v^m)_{\hat{\omega}^{0,1}}| \\ &\le \sum_{|m|=0}^{\infty} m^2 \|u^m\|_{\hat{\omega}^{0,-1}} \|v^m\|_{\hat{\omega}^{0,-1}} + \|\partial_r u^m\|_{\hat{\omega}^{0,1}} \|\partial_r v^m\|_{\hat{\omega}^{0,1}} + \alpha \|u^m\|_{\hat{\omega}^{0,1}} \|v^m\|_{\hat{\omega}^{0,1}} \\ &\le (1+\alpha)\|u\|_W \|v\|_W \quad \forall u, v \in W.\end{aligned}$$

However, it is not obvious how to prove an inf-sup condition for $A(\cdot,\cdot)$, which is required for the well-posedness of problem (2.24). We shall provide a partial answer to this problem under a special setting in the next section.

2.3. Discrete Petrov–Galerkin formulation and a practical algorithm. We now construct a discrete Petrov–Galerkin formulation for (2.24).

We first construct a spectral approximation to $\psi^m(r)$. Let $\hat{P}_N$ be the set of all polynomials on $[0,1]$ of degree no greater than N. We set $\hat{W}_N^m := \hat{W}^m \cap \hat{P}_N$, $\hat{Y}_N^m := \hat{Y}^m \cap \hat{P}_N$, and let $\{\psi_N^m\} \in \hat{Y}_N^m$ be the solution of

$$(r\partial_r \psi_N^m, \partial_r v^m) + \left(\left(\frac{m^2}{r} + \alpha r \right) \psi_N^m, v^m \right) = (r f^m, v^m) \quad \forall v^m \in \hat{Y}_N^m. \tag{2.27}$$

Then, by the superposition principle, we can check that $u_N^m = t_N^m \phi^m(r) + \psi_N^m(r)$ is the unique solution of

$$(r\partial_r u_N^m, \partial_r v^m) + \left(\left(\frac{m^2}{r} + \alpha r \right) u_N^m, v^m \right) = (r f^m, v^m) \quad \forall v^m \in \hat{Y}_N^m, \tag{2.28}$$

satisfying $u_N^m(1) = t_N^m$ in $\hat{W}_N^m$. We define the discrete trial space by

$$\begin{aligned}X_{MN} := \Bigg\{ u_{MN}(r,\theta) = \sum_{|m|=0}^{M} u_N^m(r) e^{\mathrm{i}m\theta} : u_N^m \in \hat{W}_N^m,\ \left(u_{MN}, e^{\mathrm{i}k\theta}\right)_\Gamma \\ = \left(h, e^{\mathrm{i}k\theta}\right)_\Gamma, |k| = 0, \dots, M \Bigg\}.\end{aligned} \tag{2.29}$$

Let $u_{MN} = \sum_{|m|=0}^{M} (t_N^m \phi^m(r) + \psi_N^m(r)) e^{\mathrm{i}m\theta}$, where $\{t_N^m\}$ are to be determined. Then, it is easy to see that the conditions

$$\left(u_{MN}, e^{\mathrm{i}k\theta}\right)_\Gamma = \left(h, e^{\mathrm{i}k\theta}\right)_\Gamma \text{ for } |k| = 0, \dots, M \tag{2.30}$$

are equivalent to

$$\sum_{|m|=0}^{M} \int_0^{2\pi} \left(t_N^m \phi^m(\rho(\theta)) + \psi_N^m(\rho(\theta))\right) e^{\mathrm{i}(m-k)\theta} \mathrm{d}\theta = \int_0^{2\pi} h(\rho(\theta),\theta) e^{-\mathrm{i}k\theta} \mathrm{d}\theta, \quad |k| = 0, \dots, M. \tag{2.31}$$

We set the discrete test space to be

$$Y_{MN} := \left\{ v_{MN}(r,\theta) = \sum_{|m|=0}^{M} v_N^m(r) e^{\mathrm{i}m\theta} : v_N^m \in \hat{Y}_N^m \right\}. \tag{2.32}$$

Then, our discrete Petrov–Galerkin formulation for (2.24) is

$$\begin{cases} \text{Find } u_{MN} \in X_{MN} \text{ such that} \\ A(u_{MN}, v_{MN}) = (rf, v_{MN}) \quad \forall v_{MN} \in Y_{MN}. \end{cases} \tag{2.33}$$

THEOREM 2.1. *Let* $\{\phi^m\}$ *and* $\{\phi_N^m\}$ *be the solution of* (2.10) *and* (2.27)*, respectively. Then,* (i) (2.31) *admits a unique solution* $\{t_N^m\}$*, and* (ii) $u_{MN}(r,\theta) = \sum_{|m|=0}^{M} u_N^m(r) e^{im\theta}$ *with* $u_N^m = t_N^m \phi^m(r) + \psi_N^m(r)$ *is the unique solution of* (2.33).

Proof. We first show that $\{t_N^m\}$ can be uniquely determined from (2.31). To this end, we expand $\rho(\theta)$ in Fourier series, i.e., $\rho(\theta) = \sum_{j=-\infty}^{\infty} c_j e^{\mathrm{i}j\theta}$. Note that c_0 is positive because $\rho(\theta) > 0$. Also, the expression of ϕ^m given in (2.13) implies $\{\phi^m(\rho(\theta))\}_{m=0}^{M}$ is a linearly independent set. Hence $\phi^m(\rho(\theta))e^{\mathrm{i}m\theta}$ for $|m| = 0, 1, \ldots, M$ are linearly independent. The system matrix for (2.31) is invertible since each column is the coordinate vector of $\phi^m(\rho(\theta))e^{\mathrm{i}m\theta}$ onto the finite-dimensional Fourier space.

Now we rewrite v^m in (2.28) as v^n, multiply both sides of (2.28) by $e^{\mathrm{i}(m-n)\theta}$, and integrate it with respect to θ over $[0, 2\pi)$. By summing up the results for $|m| = 0, \ldots, M$ and $|n| = 0, \ldots, M$, we find immediately that $A(u_{MN}, v_{MN}) = (rf, v_{MN})$ for all $v_{MN} \in Y_{MN}$. On the other hand, since $\{t_N^m\}$ are determined from (2.31), we find that $u_{MN} \in X_{MN}$. Hence, $u_{MN}(r,\theta)$ is a solution of (2.33).

For the uniqueness, we consider (2.33) with $f = 0$ and $h = 0$. We observe that $f = 0$ implies $\psi_N^m \equiv 0$ for all m; $h = 0$ and $\psi_N^m \equiv 0$ for all m imply that $t_N^m = 0$ for all m. Since any solution of (2.33) can be written as $u_{MN}(r,\theta) = \sum_{|m|=0}^{M} u_N^m(r) e^{im\theta}$, we have $u_{MN} = 0$. ∎

Note that the expression of solutions to (2.10) is explicitly given by (2.13). On the other hand, $\{\psi_N^m\}$ can be efficiently and accurately computed (cf. [29]); the main difficulty in finding u_{MN} is to determine $\{t_N^m\}$ from (2.31). In fact, taking $\xi_k = e^{\mathrm{i}k\theta}$ in (2.31) leads to a severely ill-conditioned linear system. However, we can reduce the condition number to a remarkable extent by using the scaled Fourier basis

$$\widetilde{\xi}_k(\theta) := \rho_{\text{avg}}^{-|k|} e^{-\mathrm{i}k\theta}, \tag{2.34}$$

where $\rho_{\text{avg}} \in (0,1)$ represents the average radius of the domain boundary. A straightforward formula for ρ_{avg} is

$$\rho_{\text{avg}} = \frac{1}{2\pi} \int_0^{2\pi} \rho(\theta) \mathrm{d}\theta. \tag{2.35}$$

Then the linear system for $\{t_N^m\}$ can be rewritten by

$$\begin{aligned} &\sum_{|m|=0}^{M} t_N^m \rho_{\text{avg}}^{-|k|} \int_0^{2\pi} \phi^m(\rho(\theta)) e^{\mathrm{i}(m-k)\theta} \mathrm{d}\theta \\ &\quad = \rho_{\text{avg}}^{-|k|} \int_0^{2\pi} h(\rho(\theta),\theta) e^{-\mathrm{i}k\theta} \mathrm{d}\theta - \rho_{\text{avg}}^{-|k|} \sum_{|m|=0}^{M} \int_0^{2\pi} \psi^m(\rho(\theta)) e^{\mathrm{i}(m-k)\theta} \mathrm{d}\theta, \ |k| = 0, \ldots, M. \end{aligned} \tag{2.36}$$

The exponentially growing factor $\rho_{\text{avg}}^{-|k|}$ added here plays the role of a preconditioner. For the trivial case $\alpha = 0$ and $\rho(\theta) = \rho_0 \in (0, 1)$, the coefficient matrix in (2.36) is exactly the identity. For general domains, our numerical examples show that the condition number of (2.36) grows exponentially as M increases, however, with a base number very close to 1. This choice of $\{\widetilde{\xi}_k\}$ leads to desirable simplicity for numerical implementation.

To summarize the preceding discussions, we propose the following algorithm.

ALGORITHM 2.1. *Given M (number of nodes in θ direction) and N (number of nodes in the r direction), we find an approximation to the extended problem* (2.2) *as follows.*

Step 1. *Compute the truncated Fourier expansion of $f(r, \theta) := F(r\cos\theta, \sin\theta)$ with respect to θ, obtaining an approximation to* (2.6).

Step 2. *Compute $\{\psi_N^m\}$ using a spectral-Galerkin method described in* [29].

Step 3. *Determine $\{t_N^m\}$ from the linear system* (2.36).

Step 4. *Compute $u_{MN}(r_k, \theta_j) = \sum_{|m|=0}^{M} u_N^m(r_k) e^{im\theta_j}$ $(0 \le k \le N,\, 0 \le |j| \le M)$ with $u_N^m(r) = t_N^m \phi^m(r) + \psi_N^m(r)$, and obtain the final approximate solution $U_{MN}(x_k, y_j) = u_{MN}(\mathbb{T}^{-1}(x_k, y_j))$ $(0 \le k \le N,\, 0 \le |j| \le M)$.*

We now estimate the computational cost for this algorithm.

Step 1. The truncated Fourier expansion of $f(r, \theta)$ can be obtained in $O(NM\log(M))$ flops using FFT.

Step 2. For each m, ϕ^m is explicitly given by (2.13), and ψ_N^m can be computed by the spectral-Galerkin formulation [29] with $O(N^2)$ flops.

Step 3. If we evaluate the integrals in (2.36) by numerical quadrature with $O(K)$ nodes and weights, then the total flops for dealing with (2.36) are $O(KMN + KM^2 + M^3)$.

Step 4. The evaluation cost by tensor product is $O(\min(N, M)NM)$.

Hence, for $K \ge M$, the complexity for Algorithm 2.1 is $O(MN^2 + KMN + KM^2)$. In particular, if we set $K = O(M)$ and $N = O(M)$, then the total complexity is $O(M^3)$, which is essentially the same order as the spectral-Galerkin algorithm for second-order elliptic equations in the rectangular domain [28]. Moreover, we should mention that the constant included in $O(\cdot)$ is small.

3. Error analysis. Analysis of the spectral approximation (2.33) in the general case appears to be very difficult, so we only consider the special case $\rho(\theta) = \rho_0$, in which the solution spaces X and X_{MN} can be characterized more explicitly. We believe that the analysis in this particular case provides some theoretical foundation for the proposed algorithm and sheds some light on the eventual analysis for the general case.

To simplify the presentation, we only consider the homogeneous boundary condition, i.e., $h = 0$. We assume $\rho_0 < 1$ and choose the extended domain to be the disk with radius 1. Also, we set $\alpha = 0$, in which case $\phi^m = r^{|m|}$. For $\alpha > 0$, $\phi^m = \frac{J_m(\sqrt{\alpha}\mathrm{i}r)}{J_m(\sqrt{\alpha}\mathrm{i})}$ will lead to similar results.

First, we define the following ρ_0-dependent subspace of $\hat{W}^m$ defined in (2.17):

$$\hat{X}^m = \{u \in \hat{W}^m : u(\rho_0) = 0\}. \tag{3.1}$$

We expand the solution of (2.24) as $u = \sum_{|m|\ge 0} u^m(r) e^{\mathrm{i}m\theta}$. In the case $\rho(\theta) = \rho_0$, $u|_{\partial\Omega} = 0$ is equivalent to $u^m(\rho_0) = 0$. Thus X in (2.22) (with $h = 0$) can be rewritten as

$$X = \left\{ u = \sum_{|m|\geq 0} u^m(r)e^{\mathrm{i}m\theta} : u^m \in \hat{X}^m, \sum_{|m|\geq 0} \|u^m\|^2_{\hat{W}^m} < \infty \right\}. \tag{3.2}$$

Similarly, let $\hat{X}^m_N = \hat{X}^m \cap \hat{P}_N$, which is a subset of $\hat{X}^m$; then

$$X_{MN} := \left\{ u_{MN} = \sum_{|m|=0}^{M} u^m_N(r)e^{\mathrm{i}m\theta} : u^m_N \in \hat{X}^m_N, |m| = 0\ldots., M \right\}. \tag{3.3}$$

Note that in this special case X_{MN} is a subspace of X.

We introduce the 1-D bilinear operator $\hat{b}_m(\cdot,\cdot) : \hat{X}^m \times \hat{Y}^m \to \mathbb{C}$ by

$$\hat{b}_m(u,v) = m^2(u,v)_{\hat{\omega}^{0,-1}} + (\partial_r u, \partial_r v)_{\hat{\omega}^{0,1}}. \tag{3.4}$$

Let $u = \sum_{|m|\geq 0} u^m(r)e^{\mathrm{i}m\theta}$ and $u_{MN} = \sum_{|m|=0}^{M} u^m_N(r)e^{\mathrm{i}m\theta}$ be the solutions to (2.24) and (2.33); then

$$\begin{cases} u^m \in \hat{X}^m \text{ such that} \\ \hat{b}_m(u^m, v^m) = (f^m, v^m)_{\hat{\omega}^{0,1}} \quad \forall v^m \in \hat{Y}^m, \end{cases} \tag{3.5}$$

and

$$\begin{cases} u^m_N \in \hat{X}^m_N \text{ such that} \\ \hat{b}_m(u^m_N, v^m_N) = (f^m, v^m_N)_{\hat{\omega}^{0,1}} \quad \forall v^m_N \in \hat{Y}^m_N, \end{cases} \tag{3.6}$$

where $\hat{Y}^m$ is defined in (2.17) and $\hat{Y}^m_N = \hat{Y}^m \cap \hat{P}_N$.

3.1. Well-posedness of the 1-D systems (3.5) and (3.6). It is easy to check that

$$|\hat{b}_m(u,v)| \leq \|u\|_{\hat{W}^m} \|v\|_{\hat{Y}^m} \ \forall m, \tag{3.7}$$

i.e., the bilinear form $\hat{b}_m(\cdot,\cdot)$ is continuous in $\hat{X}^m \times \hat{Y}^m$. For the well-posedness of (3.5) and (3.6), we need to establish an inf-sup condition for $\hat{b}_m(\cdot,\cdot)$.

First, we need the following result that estimates the boundary value for functions in $\hat{X}^m$.

LEMMA 3.1. *For $u \in \hat{X}^m$ with $\|u\|_{\hat{W}^m} = 1$, we have*

$$|u(1)| \leq \begin{cases} \hat{c}_0, & m = 0, \\ \hat{c}(\rho_0; m)|m|^{-\frac{1}{2}}, & m \neq 0, \end{cases} \tag{3.8}$$

where

$$\hat{c}_0 \approx 1.479 \quad \textit{and} \quad \hat{c}(\rho_0; m) := \left(1 - \rho_0^{2|m|}\right)^{\frac{1}{2}} \left(1 + \rho_0^{2|m|}\right)^{-\frac{1}{2}} < 1. \tag{3.9}$$

Proof. First we consider the case $m \neq 0$. We need to estimate

$$\sup |u(1)| \quad \text{s.t.} \quad \|u\|_{\hat{W}^m} = 1, \tag{3.10}$$

which is clearly equal to

$$\sup |u(1)| \quad \text{s.t.} \quad \int_{\rho_0}^1 \frac{m^2}{r}|u|^2 + r|\partial_r u|^2 \mathrm{d}r = 1, \quad u(\rho_0) = 0, \tag{3.11}$$

by taking $u \equiv 0$ in $[0, \rho_0]$ since $u(0) = 0$. Consider the following variational problem:

$$\inf \int_{\rho_0}^1 \frac{m^2}{r}|u|^2 + r|\partial_r u|^2 \mathrm{d}r \quad \text{s.t.} \quad u(\rho_0) = 0, \quad u(1) = 1. \tag{3.12}$$

The Euler–Lagrange equation of (3.12) is given by

$$\frac{m^2}{r}u - \partial_r(r\partial_r u) = 0, \quad u(\rho_0) = 0, \quad u(1) = 1, \tag{3.13}$$

whose solution is

$$u^*(r) = (1 - \rho_0^{2m})^{-1} r^m + (1 - \rho_0^{-2m})^{-1} r^{-m}. \tag{3.14}$$

Then

(3.15)

$$\begin{aligned} \inf_{u(\rho_0)=0, u(1)=1} \left(\int_{\rho_0}^1 \frac{m^2}{r}|u|^2 + r|\partial_r u|^2 \mathrm{d}r \right)^{\frac{1}{2}} &= \left(\int_{\rho_0}^1 \frac{m^2}{r}|u^*|^2 + r|\partial_r u^*|^2 \mathrm{d}r \right)^{\frac{1}{2}} \\ &= |m|^{\frac{1}{2}} \left(\left(1 - \rho_0^{2|m|}\right)^{-1} - \left(1 - \rho_0^{-2|m|}\right)^{-1} \right)^{\frac{1}{2}}. \end{aligned}$$

Hence

$$\begin{aligned} \sup_{\|u\|_{\dot{W}^m}=1} |u(1)| &= \left(\inf_{u(\rho_0)=0, u(1)=1} \left(\int_{\rho_0}^1 \frac{m^2}{r}|u|^2 + r|\partial_r u|^2 \mathrm{d}r \right)^{\frac{1}{2}} \right)^{-1} \\ &= |m|^{-\frac{1}{2}} \left(1 - \rho_0^{2|m|}\right)^{\frac{1}{2}} \left(1 + \rho_0^{2|m|}\right)^{-\frac{1}{2}}. \end{aligned} \tag{3.16}$$

Similarly for $m = 0$, we have

$$\inf_{u(\rho_0)=0, u(1)=1} \left(\int_{\rho_0}^1 (|u|^2 + |\partial_r u|^2) r \mathrm{d}r \right)^{\frac{1}{2}} = \left(\int_{\rho_0}^1 (|u^*|^2 + |\partial_r u^*|^2) r \mathrm{d}r \right)^{\frac{1}{2}}, \tag{3.17}$$

where u^* solves the Euler–Lagrange equation

$$-\partial_r(r\partial_r u) + ru = 0, \quad u(\rho_0) = 0, \quad u(1) = 1. \tag{3.18}$$

Specifically, the solution has the expression

$$u^*(r) = \frac{-K_0(\rho_0)I_0(r)}{I_0(\rho_0)K_0(1) - I_0(1)K_0(\rho_0)} + \frac{I_0(\rho_0)K_0(r)}{I_0(\rho_0)K_0(1) - I_0(1)K_0(\rho_0)}, \tag{3.19}$$

where $I_0(r)$ and $K_0(r)$ are the modified Bessel functions of the first and second kinds with $\nu = 0$. Hence by integration by parts and the property of the modified Bessel functions,

(3.20)
$$\begin{aligned}
&\sup_{\|u\|_{\hat{W}^0}=1} |u(1)| \\
&= \left(\inf_{u(\rho_0)=0,u(1)=1} \left(\int_{\rho_0}^1 (|u|^2 + |\partial_r u|^2) r \mathrm{d}r \right)^{\frac{1}{2}} \right)^{-1} \\
&= \left(\int_{\rho_0}^1 (|u^*|^2 + |\partial_r u^*|^2) r \mathrm{d}r \right)^{-\frac{1}{2}} = \left(\int_{\rho_0}^1 (-\partial_r (r \partial_r u^*) + r u^*) u^* \mathrm{d}r + \partial_r u^*(1) \right)^{-\frac{1}{2}} \\
&= (\partial_r u^*(1))^{-\frac{1}{2}} < \left(\frac{-K_0(0) I_0'(1)}{I_0(0) K_0(1) - I_0(1) K_0(0)} + \frac{I_0(0) K_0'(1)}{I_0(0) K_0(1) - I_0(1) K_0(0)} \right)^{-\frac{1}{2}} \approx 1.497.
\end{aligned}$$

The proof is complete. ∎

Also, we need the following Hardy-type inequlity.

LEMMA 3.2.

$$\int_0^1 |u(r)|^2 r \mathrm{d}r \le c_0 \int_0^1 |u'(r)|^2 r \mathrm{d}r \tag{3.21}$$

with $c_0 = \frac{1}{2}\rho_0 - \frac{1}{2}\ln \rho_0 - \frac{1}{4} > 0$ *for all* $u \in \hat{X}_0$.

Proof. Since $u(\rho_0) = 0$, we note that $u(r) = -\int_{\rho_0}^r u'(s)\mathrm{d}s$; then by the Cauchy–Schwarz inequality it follows that

(3.22)
$$\begin{aligned}
\int_0^1 |u(r)|^2 r \mathrm{d}r &= \int_0^1 \left| \int_{\rho_0}^r (u'(s) s^{\frac{1}{2}}) s^{-\frac{1}{2}} \mathrm{d}s \right|^2 r \mathrm{d}r \le \int_0^1 \left(\int_0^1 |u'(s)|^2 s \mathrm{d}s \right) \left(\int_{\rho_0}^r s^{-1} \mathrm{d}s \right) r \mathrm{d}r \\
&= \int_0^1 |u'(r)|^2 r \mathrm{d}r \int_0^1 \left(\int_{\rho_0}^r s^{-1} \mathrm{d}s \right) r \mathrm{d}r = c_0 \int_0^1 |u'(r)|^2 r \mathrm{d}r.
\end{aligned}$$

∎

We can now prove the following result.

THEOREM 3.3. *The following inequality holds:*

$$\begin{aligned}
&\inf_{u^m \in \hat{X}^m} \sup_{v^m \in \hat{Y}^m} \frac{\hat{b}_m(u^m, v^m)}{\|u^m\|_{\hat{W}^m} \|v^m\|_{\hat{W}^m}} \\
&\qquad \ge \tilde{C}(\rho_0, m) := \begin{cases} \left(\frac{1}{2}\rho_0^2 - \frac{1}{2}\ln \rho_0 + \frac{3}{4} \right)^{-1} \left(1 + \frac{\sqrt{2}}{2} \hat{c}_0 \right)^{-1}, & m = 0, \\ \rho_0^{2|m|}, & m \ne 0. \end{cases}
\end{aligned} \tag{3.23}$$

Proof. First we assume $m \ne 0$. Given $u^m \in \hat{X}^m$, suppose $\|u^m\|_{\hat{W}^m} = 1$ without loss of generality. Let $w^m = u^m(1) r^{|m|}$ and $v^m = u^m - w^m \in \hat{Y}^m$. Then by Lemma 3.1 it follows that

$$\|w^m\|_{\hat{W}^m} = |u^m(1)||m|^{\frac{1}{2}} \le \hat{c}(\rho_0; m); \tag{3.24}$$

therefore

$$\|v^m\|_{\hat{W}^m} \le \|u^m\|_{\hat{W}^m} + \|w^m\|_{\hat{W}^m} \le 1 + \hat{c}(\rho_0; m). \tag{3.25}$$

Also, since

$$\frac{m^2}{r} w^m - \partial_r (r \partial_r w^m) = 0, \tag{3.26}$$

by integrating by parts and (3.24) we have

$$\begin{aligned}(3.27)\quad \hat{b}_m(u^m, v^m) &= m^2(u^m, u^m - w^m)_{\hat{\omega}^{0,-1}} + (\partial_r u^m, \partial_r u^m - \partial_r w^m)_{\hat{\omega}^{0,1}} \\ &= \|u^m\|_{\hat{W}^m} - \int_0^1 \left(\frac{m^2}{r}\overline{w^m} - \partial_r(r\partial_r \overline{w^m})\right) u^m \mathrm{d}r - u^m(r\partial_r \overline{w^m})\Big|_0^1 \\ &= 1 - |u^m(1)|^2|m| \geq 1 - \hat{c}^2(\rho_0; m) \geq \rho_0^{2|m|}.\end{aligned}$$

Therefore, combining (3.27) and (3.25) leads to (3.23).

Similarly, we can obtain a bound for $m = 0$ by taking $v^0 = u^0 - u^0(1) \in \hat{Y}^0$ and using Lemma 3.1 and Lemma 3.2. ∎

The above result indicates that the inf-sup condition for $\hat{b}_m$ holds in the spatial continuous case. Note that in the proof of Theorem 3.3, the constructed function $v^m = u^m(r) - u^m(1)r^{|m|}$ belongs to $\hat{Y}_N^m$ if $u^m \in \hat{X}_N^m$ for $0 < |m| \leq N$, and $v^0 = u^0 - u^0(1)$ belongs to $\hat{Y}_N^0$ if $u^0 \in \hat{X}_N^0$. Hence, using exactly the same procedure as above, we can prove that the inf-sup condition holds also in the spatial discrete case.

THEOREM 3.4. *The following inequality holds:*

$$(3.28)\qquad \inf_{u^m \in \hat{X}_N^m} \sup_{v^m \in \hat{Y}_N^m} \frac{\hat{b}_m(u^m, v^m)}{\|u^m\|_{\hat{W}^m}\|v^m\|_{\hat{W}^m}} \geq \tilde{C}(\rho_0, m) \quad \forall m.$$

Remark 3.1. Notice that the inf-sup constant behaves like $\rho_0^{2|m|}$, which is a monotonically increasing function of ρ_0. Hence, it is better to choose the artificial boundary closer to the original boundary since it increases the inf-sup constant and reduces the domain for computation.

3.2. Error estimate. We introduce the orthogonal projection operator $\tilde{\pi}_N^m : \hat{W}^m \to \hat{W}_N^m$ by

$$(3.29)\qquad (\partial_r(\tilde{\pi}_N^m v - v), \partial_r w_N)_{\hat{\omega}^{0,1}} = 0 \quad \forall w_N \in \hat{W}_N^m.$$

The following approximation property of $\tilde{\pi}_N^m$ is well known (cf. Lemma 3.10 in [21]).

THEOREM 3.5. *For any $v \in \hat{W}^m \cap \hat{B}^s_{0,-1}$ with $s \geq 1$, we have*

$$(3.30)\qquad \|\tilde{\pi}_N^m v - v\|_{\hat{\omega}^{0,-1}} + \|\partial_r(\tilde{\pi}_N^m v - v)\|_{\hat{\omega}^{0,1}} \leq cN^{1-s}\|\partial_r^s v\|_{\hat{\omega}^{s,s-1}},$$

where c is a positive constant independent of m, N, and v.

In order to describe the error in $\Pi := \{(r, \theta) : \rho_0 < r < 1,\ \theta \in [0, 2\pi)\}$, we define

$$\begin{aligned}(3.31)\qquad B^s_{\mathrm{p},\rho_0}(\Pi) = \Bigg\{ u : u(r,\theta) &= \sum_{|m|=0}^{\infty} u^m(r) e^{\mathrm{i}m\theta} \text{ with } \|u\|_{B^s_{\mathrm{p},\rho_0}(\Pi)} \\ &:= \left(\sum_{|m|=0}^{\infty} \frac{1+m^2}{\tilde{C}^2(\rho_0, m)} \|\partial_r^s u^m\|^2_{\hat{\omega}^{s,s-1}}\right)^{\frac{1}{2}} < \infty \Bigg\}\end{aligned}$$

and

$$H_{\mathrm{p}}^{1,t}(\Pi)=\Bigg\{u:u(r,\theta)=\sum_{|m|=0}^{\infty}u^m(r)e^{\mathrm{i}m\theta}\ \text{with}\ u_m\in\hat{W}^m,\ \|u\|_{H_{\mathrm{p}}^{1,t}(\Pi)} \tag{3.32}$$
$$:=\left(\sum_{|m|=0}^{\infty}(1+|m|^{2t})\|u^m\|_{\hat{W}^m}^2\right)^{\frac{1}{2}}<\infty\Bigg\}.$$

We can now prove the following error estimate.

THEOREM 3.6. *Let $u\in X$ and $u_{MN}\in X_{MN}$ be the solutions of* (2.24) *and* (2.33). *Suppose $u\in B_{\mathrm{p},\rho_0}^s(\Pi)\cap H_{\mathrm{p}}^{1,t}(\Pi)$ with $s\geq 1$ and $t\geq 0$. Then*

$$\|u-u_{MN}\|_X\leq cN^{1-s}\|u\|_{B_{\mathrm{p},\rho_0}^s(\Pi)}+M^{-t}\|u\|_{H_{\mathrm{p}}^{1,t}(\Pi)}. \tag{3.33}$$

Proof. Let $u^m\in\hat{X}^m$ and $u_N^m\in\hat{X}_N^m$ be the solution of (3.5) and (3.6), respectively. By applying the second Strang lemma (Lemma 2.25 in [16]) with (3.28), it immediately follows that

$$\|u^m-u_N^m\|_{\hat{W}^m}\leq\left(1+\frac{1}{\tilde{C}(\rho_0,m)}\right)\inf_{v_N^m\in\hat{X}_N^m}\|u^m-v_N^m\|_{\hat{W}^m}\quad\forall m. \tag{3.34}$$

If in addition $u^m\in\hat{B}_{0,-1}^s$, then by Theorem 3.5, we obtain that

$$\|u^m-u_N^m\|_{\hat{W}^m}\leq c\frac{1+|m|}{\tilde{C}(\rho_0,m)}N^{1-s}\|\partial_r^s u^m\|_{\hat{\omega}^{s,s-1}}. \tag{3.35}$$

Therefore,

(3.36)
$$\begin{aligned}\|u-u_{MN}\|_X^2&=\sum_{|m|=0}^{M}\|u^m-u_N^m\|_{\hat{W}^m}^2+\sum_{|m|>M}\|u^m\|_{\hat{W}^m}^2\\&\leq c\sum_{|m|=0}^{M}\frac{1+m^2}{\tilde{C}^2(\rho_0,m)}N^{2(1-s)}\|\partial_r^s u^m\|_{\hat{\omega}^{s,s-1}}^2+M^{-2t}\sum_{|m|>M}m^{2t}\|u^m\|_{\hat{W}^m}^2\\&\leq cN^{2(1-s)}\|u\|_{B_{\mathrm{p},\rho_0}^s(\Pi)}^2+M^{-2t}\|u\|_{H_{\mathrm{p}}^{1,t}(\Pi)}^2.\end{aligned}$$

The proof is complete. ∎

4. Numerical results. To demonstrate the effectiveness of our algorithms, we present several numerical examples by using the algorithm summarized in section 2 for the linear problem (2.1), followed by a nonlinear example.

In the first example, we set $\alpha=10$ in (2.1) and consider the exact solution to be

$$U(x,y)=\exp(y/(x+2)) \tag{4.1}$$

inside a smooth domain (cf. Figure 4.1)

$$\Omega=\{(r,\theta):r<0.7+0.2\sin(3\theta)\}. \tag{4.2}$$

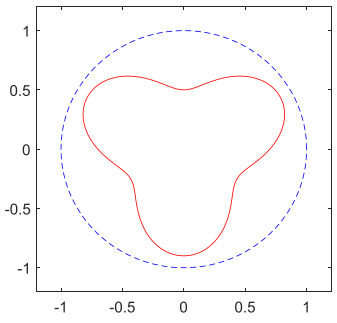

FIG. 4.1. *The original domain and the enclosing domain in the first example.*

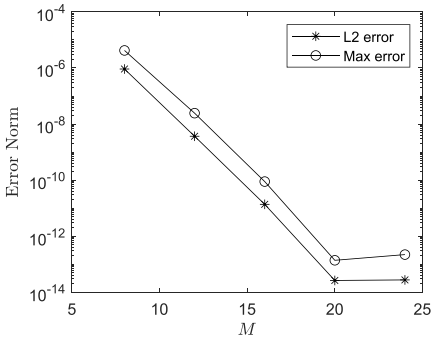

FIG. 4.2. *Relative errors versus M in the first example.*

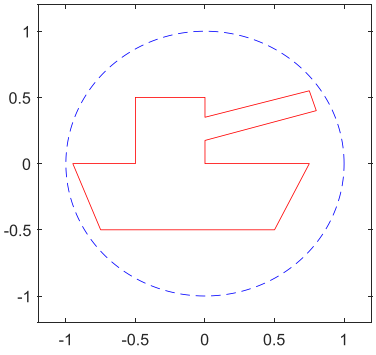

FIG. 4.3. *The original domain and the enclosing domain in the second example.*

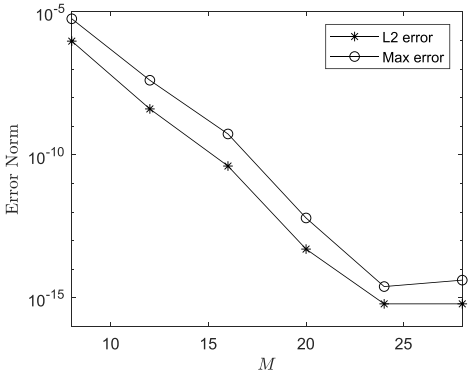

FIG. 4.4. *Relative errors versus M in the second example.*

Since the boundary is smooth, we approximate the undetermined coefficients $\{t^m\}$ by the formulation (2.31). We set $N = 2M$ and plot the relative L^2 and max errors versus M in Figure 4.2. We observe that both errors decay exponentially, which is consistent with the results in Theorem 3.6.

In the second example, we change the domain to a tank-shaped polygon (cf. Figure 4.3). The other settings are the same as the first one. The numerical results are shown in Figure 4.4. We also observe an exponential convergence rate despite the fact that the domain is not smooth.

In the third example, we consider the problem (2.1) with $F \equiv 1$ and Ω being a square $(-T, T)^2$ with $T = 0.7$, which is enclosed by a circle (cf. Figure 4.5). It is well known that the exact solution has singularities at the corners of the domain and is given by

$$u(x,y) = -\frac{64T^2}{\pi^4} \sum_{\substack{n,m=1 \\ n,m \text{ odd}}}^{\infty} (-1)^{\frac{n+m}{2}} \frac{cos(\frac{n\pi x}{2T})cos(\frac{m\pi y}{2T})}{nm(n^2+m^2)}. \tag{4.3}$$

We use the algorithm with $\{t^m\}$ being computed by (2.31) and plot the error profile in Figure 4.6, from which we see the error is mainly distributed near the four corners. In Figure 4.7, we plot the relative L^2 error versus M (with $N = 2M$). Since the solution

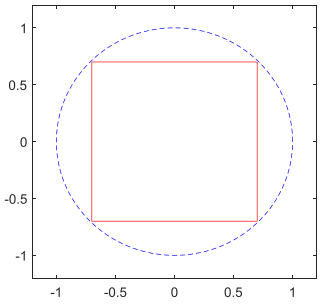

FIG. 4.5. *The original domain and the enclosing domain in the third example.*

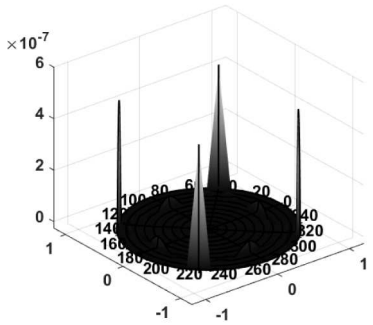

FIG. 4.6. *Error mesh when $M = 90$ in the third example.*

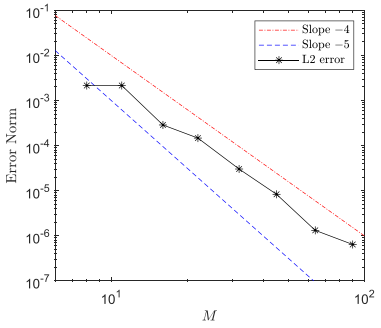

FIG. 4.7. *Relative L^2 error versus M from our spectral method in the third example.*

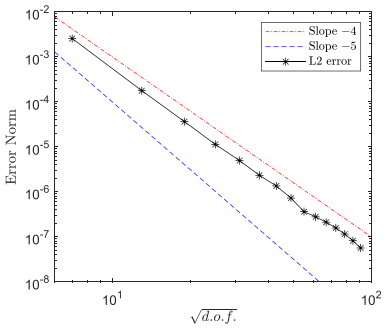

FIG. 4.8. *Relative L^2 error versus the square root of d.o.f. from spectral element method in the third example.*

has corner singularities, the convergence rate is algebraic with order between $(4, 5)$. As a comparison, we solved the same problem using the spectral element method with nine equal sized elements and plotted the convergence rate versus the square root of degree of freedom in Figure 4.8. We observe that the two methods have similar convergence rates.

As the last example, we apply our algorithm to solve the following steady-state Allen–Cahn equation:

$$\begin{aligned} -a\Delta U + U^3 - U &= F \quad \text{in } \Omega := \{(r,\theta) : r < 0.8 + 0.1\sin(5\theta)\}, \\ U &= H \quad \text{on } \partial\Omega, \end{aligned} \tag{4.4}$$

where a is a positive constant and the exact solution U is set as (4.1); the domain Ω and the enclosing circle $\tilde{\Omega}$ are shown in Figure 4.9. Assuming F is smoothly extended to $\tilde{\Omega}$, this nonlinear equation can be solved, e.g., through a fixed-point iteration

$$\begin{aligned} \alpha U_k - \Delta U_k &= -\frac{1}{a}U_{k-1}^3 + \left(\frac{1}{a} + \alpha\right) U_{k-1} + \frac{1}{a}F \quad \text{in } \tilde{\Omega}, \\ U_k &= H \quad \text{on } \partial\Omega. \end{aligned} \tag{4.5}$$

In each iteration, (4.5) is solved by our embedding method with M=32 and N=64, and the solution U_k is evaluated at radially equispaced nodes $\{(r_i, \theta_j)\}_{i=1,\ldots,N;\, j=1,\ldots,M}$.

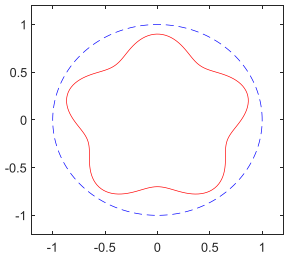

FIG. 4.9. *The original domain and the enclosing domain in the fourth example.*

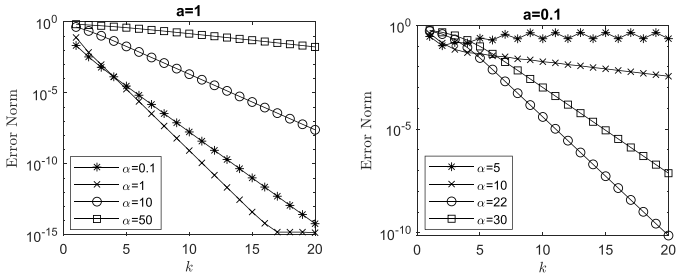

FIG. 4.10. *Relative maximum errors versus iterations in the fourth example.*

After each iteration, we will automatically get U_k in the extended domain $\tilde{\Omega}$ (at the nodes) so the right-hand side of (4.5) is well defined at the next iteration. Our numerical results indicate that good choices for α for $a = 1$ and 0.1 are 1 and 22, which lead to exponential convergence for the fixed point iteration (see Figure 4.10).

5. Extension to 3-D problems. The algorithm presented in section 2 can be extended to three dimensions by embedding the complex domain into a larger sphere. To fix the idea and simplify the presentation, we shall describe a detailed formulation in the continuous case and briefly discuss how to implement it.

Consider, for instance, the following Dirichlet problem:

$$\begin{aligned} \alpha V - \Delta V &= F \quad \text{in } \Omega, \\ V &= H \quad \text{on } \partial\Omega, \end{aligned} \tag{5.1}$$

where Ω is a 3-D domain that can be embedded in $\widetilde{\Omega} = \{(x, y, z) : \sqrt{x^2 + y^2 + z^2} < R\}$. Assuming F is smoothly extended to $\widetilde{\Omega}$, we are led to solve the extended problem

$$\begin{aligned} \alpha U - \Delta U &= F \quad \text{in } \widetilde{\Omega}, \\ U &= H \quad \text{on } \partial\Omega, \end{aligned} \tag{5.2}$$

and we have $V = U|_{\Omega}$. Now denote

$$u(r, \omega, \theta) = U(\cos\theta \sin\omega, \sin\theta \sin\omega, \cos\omega), \tag{5.3}$$

$$f(r, \omega, \theta) = F(\cos\theta \sin\omega, \sin\theta \sin\omega, \cos\omega), \tag{5.4}$$

$$h(r, \omega, \theta) = H(\cos\theta \sin\omega, \sin\theta \sin\omega, \cos\omega); \tag{5.5}$$

we can rewrite (5.2) in spherical coordinates as

$$\begin{aligned} &\alpha u - \frac{1}{r^2}\partial_r(r^2\partial_r u) - \frac{1}{r^2\sin\omega}\partial_\omega(\sin\omega\partial_\omega u) - \frac{1}{r^2\sin^2\omega}\partial_\theta^2 u = f,\\ &(r,\omega,\theta)\in(0,R)\times(0,\pi)\times[0,2\pi),\\ &u = h \quad \text{on } \Gamma, \end{aligned} \tag{5.6}$$

where Γ is the image of $\partial\Omega$ under the spherical transform.

Let $\{P_l^m\}$ be the associated Legendre functions [31] given by

$$P_l^m(x) = \frac{(-1)^m}{2^l l!}(1-x^2)^{m/2}\frac{\mathrm{d}^{l+m}}{\mathrm{d}x^{l+m}}\left\{(x^2-1)^l\right\}, \quad m\ge 0, \tag{5.7}$$

$$P_l^{-m}(x) = (-1)^m\frac{(l-m)!}{(l+m)!}P_l^m(x), \quad m<0. \tag{5.8}$$

We can expand f and u as

$$(f,u)(r,\omega,\theta) = \sum_{l=0}^{\infty}\sum_{|m|=0}^{l}(f_{lm},u_{lm})(r)P_l^m(\cos\omega)e^{\mathrm{i}m\theta}; \tag{5.9}$$

then it follows from the above and (5.6) that the coefficients $\{u_{lm}\}$ satisfy the following sequence of 1-D Bessel-type equations:

$$\begin{aligned} &\alpha u_{lm} - \frac{1}{r^2}(r^2u_{lm}')' + \frac{l(l+1)}{r^2}u_{lm} = f_{lm}, \quad r\in(0,R), \quad 0\le|m|\le l<\infty,\\ &u_{lm}(0) = 0 \ \text{ if } \ m\neq 0. \end{aligned} \tag{5.10}$$

To make the ODEs (5.10) well defined, we supplement them with the following one-sided boundary condition:

$$u_{lm}(R) = t_{lm}, \tag{5.11}$$

where the boundary values $\{t_{lm}\}$ will be determined by $u=h$ on Γ. Specifically, assuming Γ can be parametrized as $\Gamma=\{(r,\omega,\theta): r=\rho(\omega,\theta)\}$, similar to the 2-D case, we can determine $\{t_{lm}\}$ from

$$\begin{aligned} &\int_0^{2\pi}\int_0^{\pi} u(\rho(\omega,\theta),\omega,\theta;t_{lm})\overline{\xi_{kn}(\omega,\theta)}\mathrm{d}\omega\mathrm{d}\theta\\ &\quad = \int_0^{2\pi}\int_0^{\pi} h(\rho(\omega,\theta),\omega,\theta)\overline{\xi_{kn}(\omega,\theta)}\mathrm{d}\omega\mathrm{d}\theta\ \forall|n|\le k, \end{aligned} \tag{5.12}$$

where $\xi_{kn}(\omega,\theta) = P_k^n(\cos\omega)e^{\mathrm{i}n\theta}$.

Setting $u_{lm}(r) = t_{lm}\phi_l(r) + \psi_{lm}(r)$ in (5.10), we find that ϕ_l and ψ_{lm} can be uniquely determined from

$$\begin{aligned} &\alpha\phi_l - \frac{1}{r^2}(r^2(\phi_l)')' + \frac{l(l+1)}{r^2}\phi_l = 0, \quad r\in(0,R), \quad 0\le l<\infty,\\ &\phi_l(0) = 0 \ \text{ if } \ m\neq 0; \quad \phi_l(R) = 1, \end{aligned} \tag{5.13}$$

and

$$\begin{aligned} &\alpha\psi_{lm} - \frac{1}{r^2}(r^2(\psi_{lm})')' + \frac{l(l+1)}{r^2}\psi_{lm} = f_{lm}, \quad r\in(0,R), \quad 0\le|m|\le l<\infty,\\ &\psi_{lm}(0) = 0 \ \text{ if } \ m\neq 0; \quad \psi_{lm}(R) = 0\,. \end{aligned} \tag{5.14}$$

We now briefly describe the whole algorithm. Since ϕ_l, the solution of (5.13), can be expressed as the spherical Bessel function [1], we only have to find approximations to $\{\psi_{lm}(r)\}$ and $\{t_{lm}\}$.

ALGORITHM 5.1. *Given L, N, number of spherical expansion terms, and number of axial expansion terms, we find an approximation to the extended problem* (5.2) *as follows.*

Step 1. *Compute approximation to the expansion coefficients $f_{lm}(r)$ by spherical transform.*

Step 2. *Compute $\{\psi_{lm}^N\}$, approximation to $\{\psi_{lm}\}$ by solving* (5.14) *using a spectral-Galerkin method (cf.* [30]*).*

Step 3. *Determine $\{t_{lm}\}$ from the linear system*

(5.15)
$$\int_0^{2\pi}\int_0^{\pi}\sum_{l=0}^{L}\sum_{|m|=0}^{l}\left(t_{lm}\phi_l(\rho(\omega,\theta))+\psi_{lm}(\rho(\omega,\theta))\right)P_l^m(\cos\omega)e^{\mathrm{i}m\theta}\overline{\xi_{kn}(\omega,\theta)}\mathrm{d}\omega\mathrm{d}\theta$$
$$=\int_0^{2\pi}\int_0^{\pi}h(\rho(\omega,\theta),\omega,\theta)\overline{\xi_{kn}(\omega,\theta)}\mathrm{d}\omega\mathrm{d}\theta\ \forall|n|\le k\le L.$$

Step 4. *Then, the approximation to u is given by $u_{NL}(r,\omega,\theta)=\sum_{l=0}^{L}\sum_{|m|=0}^{l}u_{lm}(r)P_l^m(\cos\omega)e^{\mathrm{i}m\theta}$ with $u_{lm}(r)=t_{lm}\phi_l(r)+\psi_{lm}^N(r)$; obtain the final approximate solution $U_{NL}(x,y,z)$ from $u_{NL}(r,\omega,\theta)$ by an inverse spherical transform.*

The computational complexity can be estimated by a similar argument as in section 2.3. Step 1 costs $O(NL^3)$ flops, and Step 2 costs $O(L^2N^2)$ flops. In Step 3, suppose we evaluate the integrals in (5.15) by numerical quadrature with $O(K)$ nodes and weights for each variable; then it takes $O(K^2L^2N+K^2L^3+KL^4)$ flops to build the matrix, and we assume the linear system (5.15) is solved in X flops. And Step 4 requires $O(LN^2+L^3N)$ flops. Hence, for $K\ge L$, the complexity for Algorithm 5.1 is $O(K^2L^2N+K^2L^3+X)$. We note that $X=O(L^6)$ if (5.15) is solved with a simple Gaussian elimination but can be significantly reduced if a fast linear solver is developed. Note that the computational complexity in the 3-D case with a straightforward implementation is quite large; further investigation is needed to develop a more efficient implementation.

6. Concluding remarks. This paper developed an efficient spectral method for solving elliptic problems in complex domains using a domain embedding approach. By inserting the original complex domain into a regular circular domain, the extended problem, under a Petrov–Galerkin formulation, can be decomposed into a sequence of 1-D problems with undetermined boundary conditions at the outer artificial boundary. Then, the undetermined boundary conditions can be uniquely determined using the original boundary condition. The complete algorithm is very efficient and easy to implement. More precisely, in the 2-D case, it only requires solving a sequence of 1-D Bessel-type problems that can be efficiently solved by a spectral-Galerkin method, plus a system with unknowns being the undetermined boundary conditions. Compared to the approach of embedding complex domains into a rectangular domain, the approach with circular embedding is much more efficient and more comfortable to implement.

We also presented several numerical results to show that our algorithm can achieve exponential convergence if the solution of the original problem is smooth, regardless of whether the domain boundary is smooth or not. However, for problems with corner

singularities, it only leads to algebraic convergence rates similar to that achieved by a spectral element method on the original domain.

The main difficulty for the well-posedness and error analysis of the proposed approach is to prove a uniform inf-sup condition for the Petrov–Galerkin formulation. As a first step towards error analysis for general situations, we provided in this paper a complete analysis of the special case where the original domain is a circle. A delicate analysis was carried out to estimate the inf-sup constants, which in turn lead to error estimates. Then, by using the general framework for the transformed field expansion method presented in [25], one should be able to extend the analysis to more general domains that can be regarded as perturbations of circular domains. In future work, we shall carry out a rigorous analysis for general domains as well as applications of this approach to other problems such as the Helmholtz equation for acoustic scattering.

REFERENCES

[1] M. Abramowitz, I. A. Stegun, and R. H. Romer, *Handbook of Mathematical Functions with Formulas, Graphs, and Mathematical Tables*, Dover, New York, 1964.

[2] B. Adcock, D. Huybrechs, and J. Martin-Vaquero, *On the numerical stability of Fourier extensions*, Found. Comput. Math., 14 (2014), pp. 635–687.

[3] N. Albin and O. P. Bruno, *A spectral FC solver for the compressible Navier-Stokes equations in general domains* I*: Explicit time-stepping*, J. Comput. Phys., 230 (2011), pp. 6248–6270.

[4] N. Albin, O. P. Bruno, T. Y. Cheung, and R. O. Cleveland, *Fourier continuation methods for high-fidelity simulation of nonlinear acoustic beams*, J. Acous. Soc. Amer., 132 (2012), pp. 2371–2387.

[5] P. Angot, C.-H. Bruneau Pan, and P. Fabrie, *A penalization method to take into account obstacles in incompressible viscous flows*, Numer. Math., 81 (1999), pp. 497–520.

[6] K. E. Atkinson, *The Numerical Solution of Integral Equations of the Second Kind*, Cambridge Monogr. Appl. Comput. Math. Cambridge University Press, Cambridge, UK, 1997.

[7] J. P. Boyd, *A comparison of numerical algorithms for Fourier extension of the first, second, and third kinds*, J. Comput. Phys., 178 (2002), pp. 118–160.

[8] C. A. Brebbia, J. C. F. Telles, and L. C. Wrobel, *Boundary Element Techniques: Theory and Applications in Engineering*, Springer-Verlag, Cham, 1984.

[9] O. P. Bruno and M. Lyon, *High-order unconditionally stable FC-AD solvers for general smooth domains* I*. Basic elements*, J. Comput. Phys., 229 (2010), pp. 2009–2033.

[10] A. Bueno-Orovio and V. M. Perez-Garcia, *Spectral smoothed boundary methods: The role of external boundary conditions*, Numer. Methods Partial Differential Equations, 22 (2005), pp. 435–448.

[11] A. Bueno-Orovio, V. M. Perez-Garcia, and F. H. Fenton, *Spectral methods for partial differential equations in irregular domains: The spectral smoothed boundary method*, SIAM J. Sci. Comput., 28 (2006), pp. 886–900.

[12] Q. V. Dinh, R. Glowinski, J. He, V. Kwock, T. W. Pan, and J. Periaux, *Lagrange multiplier approach to fictitious domain methods: Application to fluid dynamics and electromagnetics*, in Domain Decomposition Methods for Partial Differential Equations, D. E. Keyes, T. F. Chan, G. Meurant, J. S. Scroggs, and R. G. Voigt, eds., SIAM, Philadelphia, 1992.

[13] S. Duczek and U. Gabbert, *Efficient integration method for fictitious domain approaches*, Comput. Mech., 56 (2015), pp. 725–738.

[14] S. Duczek, S. Liefold, and U. Gabbert, *The finite and spectral cell methods for smart structure applications: Transient analysis*, Acta Mech., 226 (2015), 845–869.

[15] M. Elghaoui and R. Pasquetti, *A spectral embedding method applied to the advection-diffusion equation*, J. Comput. Phys., 125 (1996), pp. 464–476.

[16] A. Ern and J.-L. Guermond, *Theory and Practice of Finite Elements*, Springer, Cham, 2004.

[17] D. Giraldo and D. Restrepo, *The spectral cell method in nonlinear earthquake modeling*, Comput. Mech., 60 (2017), 883–903.

[18] R. Glowinski, T.-W. Pan, and J. Periaux, *A fictitious domain method for Dirichlet problem and applications*, Comput. Methods Appl. Mech. Engrg., 111 (1994), pp. 283–303.

[19] W. J. Gordon and C. A. Hall, *Transfinite element methods: Blending-function interpolation over arbitrary curved element domains*, Numer. Math., 21 (1973/74), pp. 109–129, https://doi.org/10.1007/BF01436298.

[20] Y. Gu and J. Shen, *Accurate and efficient spectral methods for elliptic PDEs in complex domains*, J. Sci. Comput., 83 (2020), p. 42, https://doi.org/10.1007/s10915-020-01226-9.
[21] B.-y. Guo and L.-l. Wang, *Jacobi approximations in non-uniformly Jacobi-weighted Sobolev spaces*, J. Approx. Theory, 128 (2004), pp. 1–41.
[22] X. Li, J. Lowengrub, A. Ratz, and A. Voigt, *Solving PDEs in complex geometries: A diffuse domain approach*, Commun. Math. Sci., 7 (2009), pp. 81–107.
[23] M. Lyon, *A fast algorithm for Fourier continuation*, SIAM J. Sci. Comput., 33 (2011), pp. 3241–3260.
[24] M. Lyon and O. P. Bruno, *High-order unconditionally stable FC-AD solvers for general smooth domains* II. *Elliptic, parabolic and hyperbolic PDEs; theoretical considerations*, J. Comput. Phys., 229 (2010), pp. 3358–3381.
[25] D. P. Nicholls and J. Shen, *A rigorous numerical analysis of the transformed field expansion method*, SIAM J. Numer. Anal., 47 (2009), pp. 2708–2734, https://doi.org/10.1137/080741914.
[26] S. A. Orszag, *Spectral methods for problems in complex geometries*, J. Comput. Phys., 37 (1980), pp. 70–92, https://doi.org/10.1016/0021-9991(80)90005-4.
[27] K. Schneider, *Numerical simulation of the transient flow behaviour in chemical reactors using a penalisation method*, Comput. & Fluids, 34 (2005), pp. 1223–1238.
[28] J. Shen, *Efficient spectral-Galerkin method* I. *Direct solvers for second- and fourth-order equations by using Legendre polynomials*, SIAM J. Sci. Comput., 15 (1994), pp. 1489–1505.
[29] J. Shen, *Efficient spectral-Galerkin methods.* III. *Polar and cylindrical geometries*, SIAM J. Sci. Comput., 18 (1997), pp. 1583–1604, https://doi.org/10.1137/S1064827595295301.
[30] J. Shen, *Efficient spectral-Galerkin methods.* IV. *Spherical geometries*, SIAM J. Sci. Comput., 20 (1999), pp. 1438–1455, https://doi.org/10.1137/S1064827597317028.
[31] G. Szegö, *Orthogonal Polynomials*, Amer. Math. Soc. Collog. Publ. 23, American Mathematical Society, Providence, RI, 1939.
[32] R. N. van yen, D. Kolomenskiy, and K. Schneider, *Approximation of the Laplace and Stokes operators with Dirichlet boundary conditions through volume penalization: A spectral viewpoint*, Numer. Math., 128 (2014), pp. 301–338.
[33] R. Zamolo, L. Parussini, and V. Pediroda, *The finite and spectral cell methods for smart structure applications: Transient analysis*, J. Sci. Comput., 74 (2018), p. 805–825.